

The fracture of particulate-filled epoxide resins

Part 1

A. C. MOLONEY, H. H. KAUSCH

Ecole Polytechnique Fédérale de Lausanne, Laboratoire de Polymères, 32, chemin de Bellerive, CH-1007 Lausanne, Switzerland

H. R. STIEGER

Brown Boveri & Cie. AG, Zentrallabor, Abt. Kunststoffe, Affolternstrasse 52, CH-8050 Zürich-Oerlikon, Switzerland

The fracture properties of two commercial epoxide resins have been investigated both unfilled and filled with varying volume fraction of silica, alumina and dolomite particles. The values of the stress intensity factor, K_{IC} , at a certain crack velocity, were measured using the double torsion test technique. In selected cases comparative values were obtained using the single-edge notch geometry. In order to examine the influence of the resin-filler adhesion on the fracture toughness, alumina particles were treated with three silane compounds changing the degree of adhesion between the phases. The yield stresses and flexural strengths of the composites were also measured. The changes in fracture toughness in the presence of the inclusions have been explained in terms of a crack pinning mechanism.

1. Introduction

Particulate fillers are incorporated into plastic components principally because of their low cost. However, in certain cases mechanical [1], thermal [2] and electrical properties [3] may be improved, notably the elastic modulus [4], heat distortion temperature [5-7] and the dielectric strength [8].

Considerable work has been reported in the literature on the effect of particulate fillers on the mechanical properties of thermoplastic and thermosetting polymers but the underlying mechanisms are still unclear. Since the cost of plastics continues to rise at a rate faster than that of mineral fillers, it is of great importance that fillers and surface treatments for specific applications be chosen on a more rational basis.

In this paper we have investigated the fracture properties of two commercial epoxide resins filled with alumina, silica and dolomite particles. The principal parameters which have been varied are volume fraction, filler surface treatment, mechanical resistance of the filler and particle size. An attempt has been made to relate the

changes in mechanical properties with the underlying mechanisms involved.

2. Materials and experimental details

Two commercial epoxide resins were used in this investigation. The first (Resin A) was solid at room temperature and based on the diglycidyl ether of bisphenol-A cured with phthalic anhydride. The second (Resin B) was an epoxide based on dimethylhydantoin which was also anhydride cured. The curing conditions were followed in accordance with the manufacturers instructions. After being thoroughly mixed, the resins were degassed and poured into pre-heated steel moulds which were rotated, if necessary, to prevent sedimentation. Alumina, silica and dolomite fillers were used; the salient physical properties are shown in Table I.

Unlike silica, alumina is not available pre-treated with a silane coupling agent. Thus, the alumina particles were treated with three silane compounds in order to alter the adhesion between the phases. The first, hexamethyl-di-silazane (HMDS), would be expected to reduce the

TABLE I Properties of filler materials

Filler	Specific gravity (g cm ⁻³)	Form of particles	Mean particle size (μm)	Young's modulus (GPa)	Fracture toughness, K_{IC} (MN m ^{-3/2})	Work of fracture, G_{IC} (J m ⁻²)
Alumina	3.97	irregular-rounded edges	~ 6	320 [16]	5.3 [13]	40 [19]
Silica	2.65	irregular-sharp edges	W 10 ~ 60 W 6 ~ 100 W 4 ~ 160 W 1 ~ 300	94 [17]	0.8 [18]	4.4 [18]
Dolomite	2.85	irregular-sharp edges	~ 20	78 [17]	—	—

adhesion. The other two compounds were both commercial silane "coupling agents" γ aminopropyltriethoxysilane (A1100*) and γ glycidoxypropyltriethoxysilane (A187*) and would be expected to improve the resin-filler adhesion. The filler particles were treated using a technique based on that suggested by Trachte and DiBenedetto [9]. In order to estimate the level of absorption of the silanes a carbon analysis was carried out on both treated and untreated fillers.

The double torsion test technique was employed in order to measure the stress intensity factors of these composites. Certain authors [10–12] have questioned the validity of this geometry owing to the curved front which is produced. However, the difficulty of machining these highly filled resins prevented the use of another geometry. (In a few selected cases comparative values were obtained by using single-edge notch specimens). The stress intensity factors were measured using both the constant cross-head displacement rate and the load-relaxation methods [13].

The relationship between, K_{IC} , and the applied load P , is shown below.

$$K_{IC} = W_n P \left[\frac{1 + \nu}{W t^3 t_n k_1} \right]^{1/2} \quad (1)$$

where W_n is the moment arm, ν Poisson's ratio, W the specimen width, t the specimen thickness, t_n is the specimen thickness in the plane of the crack, and k_1 is a geometric factor.

Crack velocities were determined by a technique developed in our laboratories by Stalder and Beguelin [14] employing the change in the inverse of resistance with time of a thin layer of carbon applied to the specimen by means of a spray.

The two sections of the double torsion specimen after failure were used to measure the flexural strength by a three-point bending test. Three faces of the specimen were polished to eliminate surface flaws. For Resin B filled with 30% untreated alumina and 30% alumina treated with A187, the tensile strengths were also measured.

The yield stresses (σ_y) of the composites were determined using the plane strain compression test developed by Williams and Ford [15]. Employing this test permitted the use of the failed values of the double torsion specimens enabling K_{IC} and σ_y to be compared for the same sample.

3. Results and discussion

Unfilled Resin A exhibited unstable (or stick-slip) crack propagation at low cross-head speeds and, thus, two values of K_{IC} appropriate to crack initiation (K_{II}) and to crack arrest (K_{Ia}) were derived. At higher cross-head speeds the propagation became stable. As observed by Gledhill *et al.* [20] for certain other epoxide resins, the value of K_{Ia} was essentially independent of the cross-head displacement rate and the same as the value of K_{IC} for stable propagation. We have chosen, therefore, K_{Ia} to be the characteristic stress intensity factor of this material.

In contrast Resin B showed stable crack propagation in the range of cross-head speeds investigated and a linear relationship between K_{IC} and cross-head rate was observed. The presence of silica and alumina particles at levels of above 20% by volume resulted in stable propagation for both resin systems at 20°C. At 85°C, however, Resin A filled with 30% by volume of silica showed unstable crack propagation.

Kinloch and Williams [21] have explained the transition from stable to unstable crack propagation

*Trademark of Union Carbide.

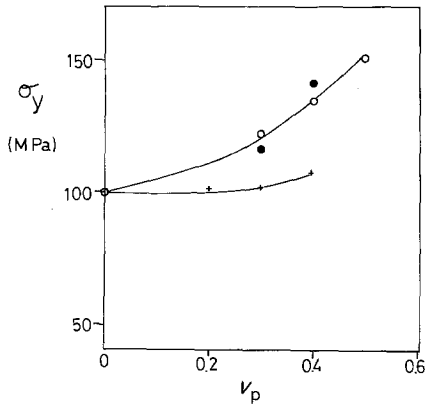


Figure 1 The variation in yield stress with volume fraction of filler. Resin B: ● alumina, ○ silica, + dolomite.

in the following manner. For resins with a low yield stress (σ_y) (100 MPa appears to be a critical value) material in the vicinity of the crack tip may flow whilst the crack is propagating and cause crack-tip blunting. A larger stress is necessary to recreate a sharp crack and hence the value of K_{II} is greater than that of K_{Ia} . Yamini and Young [22] have shown that the yield stress of epoxides increases linearly with increasing cross-head displacement rate.

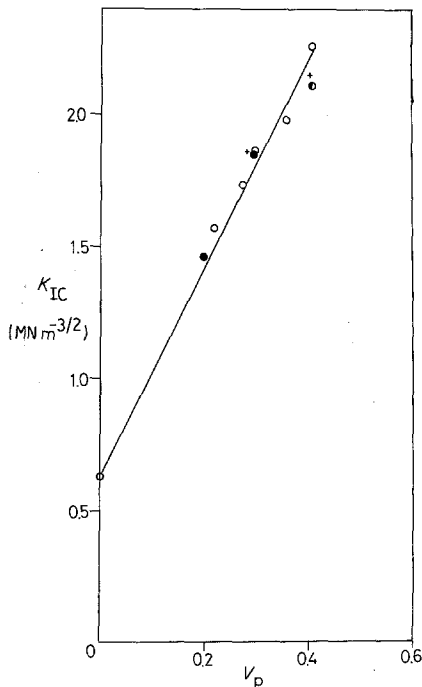


Figure 2 The variation in stress intensity factor with volume fraction of filler. Resin A: ○ alumina (DT), ● silica (DT), ○ silane treated silica (DT), + silica (SEN test).

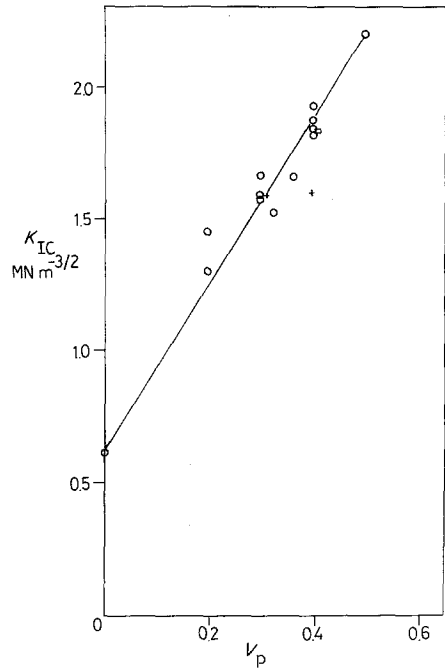


Figure 3 The variation in stress intensity factor with volume fraction of filler. Resin B: ○ alumina (DT), ● silica (DT), ○ silane treated silica (DT), + silica (SEN test), □ alumina (SEN test).

Pure Resin A was found to have a yield stress inferior to 100 MPa (cross-head speed 0.025 min^{-1}) whereas that of resin B is at this limit. Inclusion of silica and alumina particles leads to an increase in σ_y with the volume fraction of filler as shown in Fig. 1. Heating the resin results in a decrease in the yield stress and, for example, a composite prepared from Resin A filled with 30% silica had a yield stress at 85°C of 80 MPa. This composite showed unstable crack propagation. Thus it appears that the criterion developed by Kinloch and Williams [21] is also valid for filled epoxide resins since in all cases where unstable crack propagation was observed the yield stress of the material was lower than 100 MPa.

The relationship between K_{IC} and volume fraction of filler was found to be linear for both resins as shown in Figs 2 and 3. For a given resin the data for silica and alumina may be superimposed. This result is surprising firstly, because of the dissimilarity in particle size of the two fillers and secondly, because of the discrepancy in elastic moduli of these two filler materials (see Table I). Thirdly, the appearance of the fracture surfaces under the scanning electron

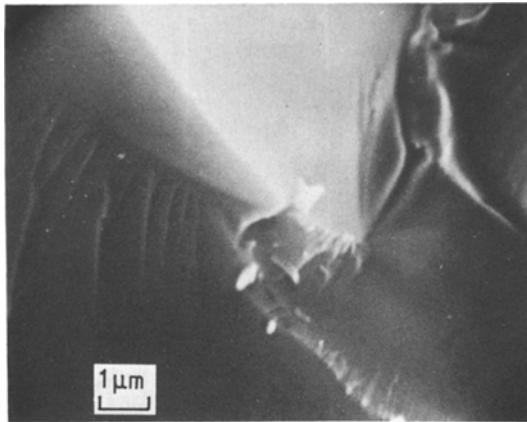


Figure 4 Scanning electron micrograph of the fracture surface of Resin B containing 40% by volume of silica.

microscope was completely different. The silica particles were well-bonded to the resin whereas each alumina particle was clearly de-bonded from the resin (see Figs. 4 and 5). These results suggest that for these irregularly shaped and relatively “strong” particles neither the particle size at a constant volume fraction of filler nor the particle–filler adhesion greatly influences the toughness.

In order to investigate the former parameter, silica was chosen since this is readily available in a wide range of particle sizes. The mean particle size was varied between ~ 300 and $\sim 60 \mu\text{m}$. As can be seen from Table II the stress intensity factor was little affected at a constant volume fraction of filler.

To determine the effect of resin–particle adhesion on the fracture toughness alumina filled resins were chosen. For both resin systems

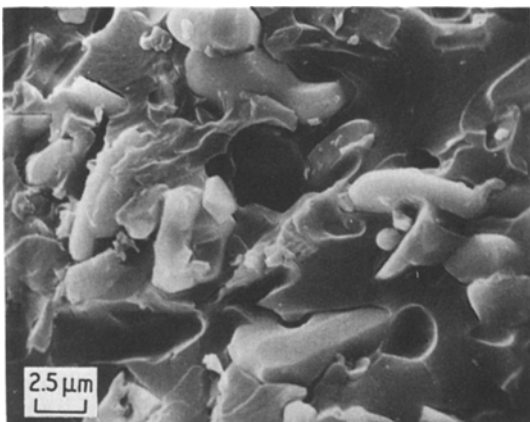


Figure 5 Scanning electron micrograph of the fracture surface of Resin B containing 40% by volume of untreated alumina.

TABLE II The influence of filler particle size on the stress intensity factor Resin B + 40% SiO_2

Grade of quartz	Mean particle size (μm)	Mean value of K_{IC} ($\text{MN m}^{-3/2}$)
W 1	~ 300	1.76 ± 0.01
W 4	~ 160	1.74 ± 0.02
W 6	~ 100	1.87 ± 0.01
W10	~ 60	1.83 ± 0.02

treatment with the silanes A1100 and A187 increased the fracture toughness as compared with the untreated material. Conversely treatment with HMDS decreased this value. However, the differences were not large and, compared to the unfilled resin, are negligible. The value of K_{IC} for pure Resin B is $\sim 0.6 \text{MN m}^{-3/2}$ and with 30% by volume of filler this is increased to between 1.46 and $1.67 \text{MN m}^{-3/2}$ irrespective of the filler surface treatment (Table III). Scanning electron micrographs of the fracture surfaces are shown in Figs 6 to 8. Treatment of the filler by HMDS resulted in a fracture surface (Fig. 6) very similar to that observed for the untreated filler (Fig. 5). Treatment of alumina with A187 improved markedly the adhesion between the resin and the filler, as demonstrated in Fig. 7. For the alumina treated with the silane A1100 some particles were well-bonded and others poorly bonded as shown in Fig. 8.

Broutman and Sahu [23] have reported an investigation of the fracture toughness of a glass bead-filled epoxide using the double cantilever beam test method. The glass beads were treated with two commercial silane “coupling agents” and a resinous silicone containing a high proportion of dimethylsiloxane which was intended to act as a mould release agent. The results were compared with untreated glass. At levels of 30%

TABLE III Stress intensity factor of composites filled with treated and untreated fillers

Filler	Treatment	Mean value, K_{IC} ($\text{MN m}^{-3/2}$)
<i>Resin A</i>		
30% alumina	none	1.86 ± 0.01
	HMDS	1.80 ± 0.01
	A187	1.97 ± 0.04
	A1100	1.99 ± 0.04
<i>Resin B</i>		
30% alumina	none	1.53 ± 0.02
	HMDS	1.46 ± 0.04
	A187	1.64 ± 0.01
	A1100	1.67 ± 0.02

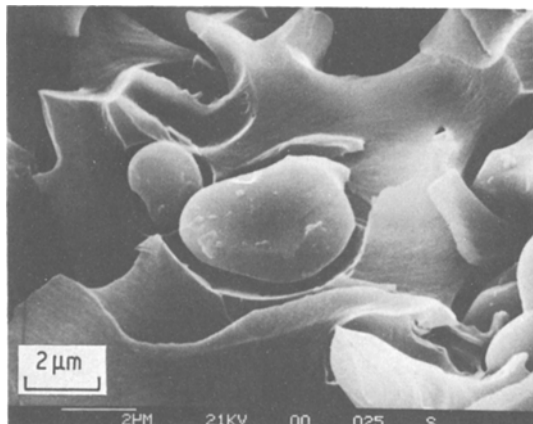


Figure 6 Scanning electron micrograph of the fracture surface of Resin A containing 30% by volume of alumina treated with HMDS.

by volume of glass, unstable crack propagation was observed for all treatments. At 50% by volume, stable propagation occurred in all cases. Considering more closely the values for 50% volume fraction, the fracture toughnesses were the same, within experimental scatter, for untreated beads and those treated with silane “coupling agents”. In contrast, the treatment with the silicone resin doubled the fracture toughness. In that report no details of the method used to treat the filler was given and no estimation of the level of treatment. It must, therefore, be considered that the silicone may not only act as a debonding agent between the resin and the filler but also may be present in sufficient quantity to plasticize the resin. The fracture surface for the silicone treated glass was considerably rougher than for the other treatments.

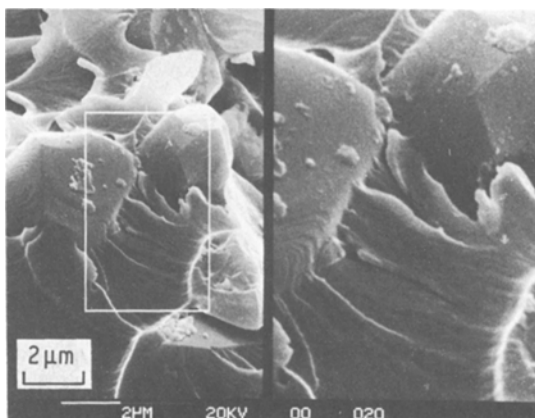


Figure 7 Scanning electron micrograph of the fracture surface of Resin B containing 30% by volume of alumina treated with A187.

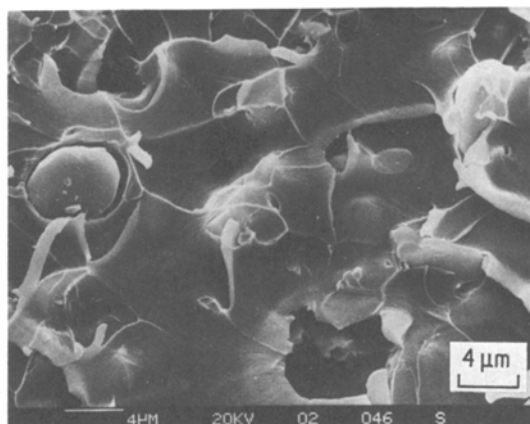


Figure 8 Scanning electron micrograph of the fracture surface of Resin A containing 30% by volume of alumina treated with A1100.

Hammond and Quayle [24] have reported a similar study for a glass-filled polyester resin. They used untreated beads, beads treated with a “coupling agent” and with an intermediate treatment and found that the “coupled” system was the toughest. This is in agreement with the results described here for the alumina-filled resin.

We have also conducted some tests on composites using glass beads, and this work will be reported in detail in a separate publication. Spherical glass beads give composites with properties somewhat different to the irregularly shaped silica and alumina particles. If the beads are well-bonded to the matrix the composite has a yield stress that is greater than that of the resin. However, if the beads are poorly bonded the yield stress is inferior to that of the resin and crack propagation is unstable.

For the silica and alumina-filled resins the presence of filler particles provokes a large increase in toughness which is independent of the resin–particle adhesion. There are a number of possible mechanisms for this phenomenon. Firstly, the toughness may be increased by the filler diverting the crack and causing a larger surface area of fracture. However, the increase in area is insufficient to account for the large rise in toughness. Secondly, in the case of some filled systems, using, for example, metallic or rubber particles [25], energy may be absorbed by deformation of the filler thus causing the observed increases in toughness. This mechanism is not for brittle glass and ceramic fillers. Thirdly, the increase in toughness may arise from an increased plastic deformation of the matrix. Fourthly, the

augmentation may be due to the obstacles pinning the crack and causing the crack front to bow out between the particles.

This latter explanation was put forward by Lange [26] who said that the increase in fracture energy was proportional to the inverse of the interparticle spacing ($2c$). He proposed an equation of the form:

$$\gamma_{\text{comp}} = \gamma_{\text{res}} + \frac{T}{2c} \quad (2)$$

where γ_{comp} and γ_{res} are the fracture energies of the composite and pure resin, respectively, and T is the line tension effect. However, this analysis is not directly applicable as T is a function of the particle size ($2r$). For a penny-shaped crack Lange deduced that the line energy was:

$$T = \frac{2r}{3} (\gamma_{\text{res}}). \quad (3)$$

The ratio of the particle size to the particle spacing is proportional to the volume fraction V_p by $[V_p/(1 - V_p)]$. Thus, Lange's equation predicts a linear relationship between the fracture energy and the ratio of r to c . However, this linear correlation has not been observed in practice except for the case of a ceramic composite, glass-filled alumina [27]. For particulate-filled plastics such a linear dependence is not found. The strain energy release rate ($G_{\text{IC}} = 2\gamma$) is related to the stress intensity factor as follows:

$$G_{\text{IC}} = \frac{K_{\text{IC}}^2(1 - \nu^2)}{E} \quad (4)$$

where E is Young's modulus.

The increase in E with volume fraction is well-known to be a complex function of the moduli of the two phases, and a parabolic relationship is found [28–30]. An example of the change in E with volume fraction is shown in Fig. 9. The effect that E rises at a faster rate than K_{IC} with increasing volume fraction of filler means that even for "strong" fillers the value of G_{IC} will go through a maximum at a certain volume fraction. An example of the relationship between G_{IC} and V_p is shown in Fig. 10, a very similar result has been obtained by Young and Beaumont [31, 32]. The analysis of Lange was carried further by Evans [33] who calculated the increase in strain energy necessary to bow out the crack between the particles. Evans also calculated the ratio of G_{IC} of the composite to that of the resin

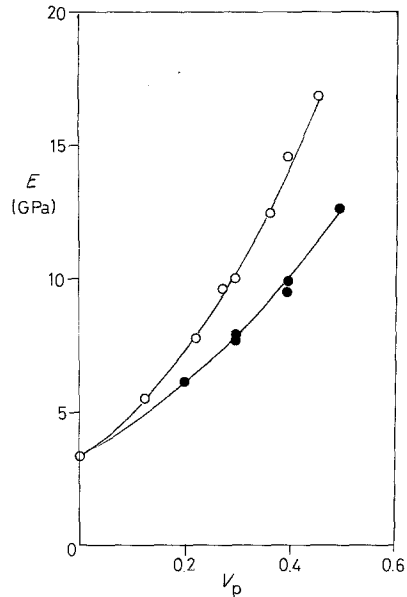


Figure 9 The variation in Young's modulus with volume fraction of filler. Resin B: ● silica, ○ alumina.

or the ratio of the tensile strength of the composite to that of the resin. Attempts to predict changes in tensile strength in this manner are problematic because the presence of the second-phase inclusions increases the size of the "inherent flaws" even if the adhesion between resin and filler is good. The flexural and tensile strengths of the alumina-filled resins are shown in Table IV. The strengths were greatly improved by treatment with A187 and A1100 and impaired by the HMDS treatment. The tensile strength and the stress intensity factor are related as follows:

$$K_{\text{IC}} = Y\sigma a^{1/2}, \quad (5)$$

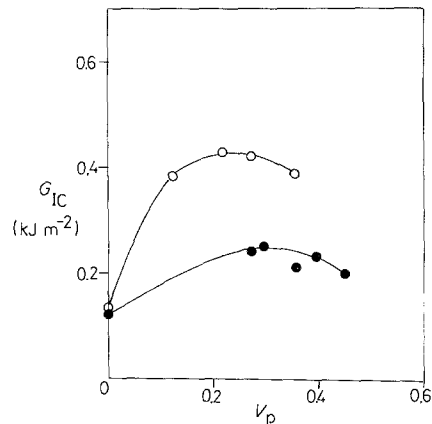


Figure 10 The variation in the strain energy release rate with volume fraction of filler. ○, Resin A + alumina; ●, Resin B + alumina.

TABLE IV Strengths of composites made from treated and untreated fillers

Resin	Filler	Treatment	Flexural strength (MPa)	Tensile strength (MPa)
B	30% alumina	none	95.7	45
		HMDS	82.2	—
		A187	131.9	87.8
		A1100	136.2	—
A	30% alumina	HMDS	106.8	—
		A1100	144.9	—
		A187	154.7	—

where Y is a geometric factor and a the effective “inherent flaw” size.

The tensile strength must be used here since the flexural strengths are too close to the yield point. Inserting the relevant values into this equation gives a flaw size of $400\ \mu\text{m}$ for Resin B filled with 30% untreated alumina and $100\ \mu\text{m}$ for this resin with 30% A187 treated alumina. Thus, even for a composite with well-bonded particles the effective flaw size is greater than that of the pure resin, which is about $50\ \mu\text{m}$. The very large flaw size for composites prepared from untreated alumina probably arises from the linking of poorly bonded particles (see Fig. 11). Radford [34] has also calculated flaw sizes of this order of magnitude for a filled epoxide resin which he attributed to trapped air. However, air bubbles of this size ($400\ \mu\text{m}$) would be clearly visible to the naked eye and careful specimen preparation avoids this problem, in particular at low filler content.

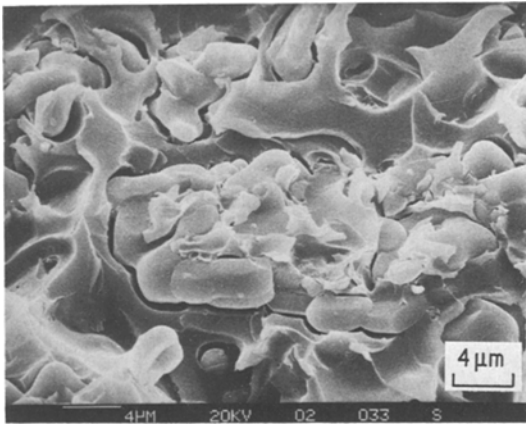


Figure 11 Scanning electron micrograph of the fracture surface of a tensile specimen prepared using untreated alumina – debonded particles may link up to form larger flaws.

Evans [33] has calculated the relative tensile strength in the presence of inclusions, $\sigma_{\text{composite}}/\sigma_{\text{resin}}$, assuming that the flaw size is constant. This is clearly invalid for these composites since we have seen that changing the adhesion between the phases alters the flaw size. However, from Equation 5, if a is constant the ratio obtained by Evans can be used directly as the ratio of the stress intensity factors: $K_{\text{IC, composite}}/K_{\text{IC, resin}}$. The increase in strain energy (U) due to the crack is:

$$U = \frac{-16(1-\nu^3)c^3(\sigma_A^s)^2}{\pi E} \int_0^{\pi/2} \left[\int_0^{\pi/2} \left(1 + \frac{c'}{2r_0 + 2c \sin \theta \sin \beta} \right)^{1/2} d\beta \right]^2 \times \sin \theta d\theta - U_0 \quad (6)$$

where σ_A^s is the stress required to propagate a crack through a series of obstacles and θ and β are defined in Fig. 12. Thus, differentiating U with respect to c and carrying out a numerical integration of the double integral, the ratio of $K_{\text{IC, composite}}/K_{\text{IC, resin}}$ may be obtained. These calculations have been carried out by Green *et al.* [35]. The values derived from this analysis are shown in Fig. 13 and compared with the experimental values for Resins A and B filled with silica and alumina. At low filler contents the theoretical values are in very good agreement, at higher volume fractions there is some scatter. This probably arises because the crack front bows out in a semi-elliptical manner rather than in a semi-circular [35]. However, this analysis shows that the increase in stress intensity factor of these resins filled with silica and alumina particles may be explained by a mechanism of crack pinning.

The mechanism proposed by Lange [26] and Evans [33] is clearly invalid in the case of weak particles. For the dolomite-filled resins it was

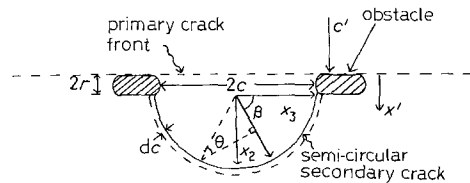


Figure 12 A semi-circular flaw at the “breakaway” position. dc is an increment in crack length at fracture (after Evans [33]).

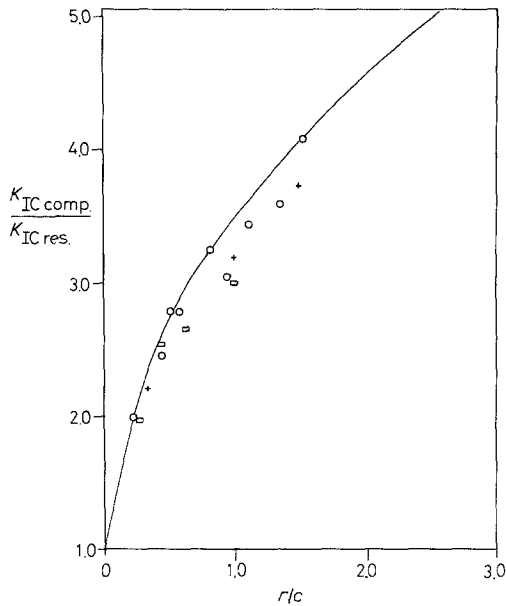


Figure 13 The increase in stress intensity factor required to move a semi-circular crack through a series of obstacles: — theoretical curve; ○, Resin A + silica; ●, Resin A + alumina; □ Resin B + alumina; + Resin B + silica.

found that above a certain critical volume fraction (~ 20%) a plateau is reached and the stress intensity factor no longer increases (see Fig. 14). This appears to be due to propagation of cracks through the particles. Some evidence in favour of this explanation was provided from scanning electron microscopy of the fracture surface (see Fig. 15). Lange and Radford [36] have studied the toughness of an aluminium hydroxide-filled

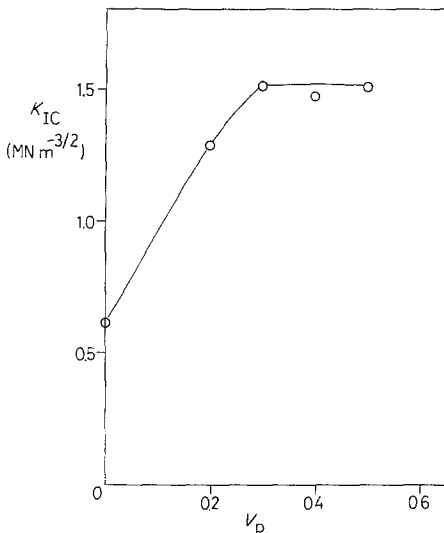


Figure 14 The variation in stress intensity factor with volume fraction of filler. Resin B + dolomite.

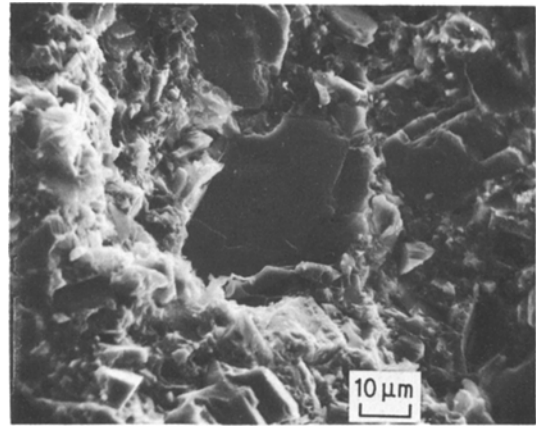


Figure 15 Scanning electron micrograph of the fracture surface of Resin B containing 40% by volume of dolomite.

epoxide resin. This filler, like dolomite, consists of relatively weak particles. Calculating from their data the relationship between K_{IC} and V_p a plateau is obtained, analogous to that reported here. Thus, for these two fillers it is highly probable that this plateau is caused by trans-particle fracture. In contrast to our results for silica, Lange and Radford found that the toughness was dependent upon the particle size of the aluminium hydroxide. However, it is comprehensible that for these “weak” fillers the particle size could affect the point at which trans-particle fracture occurs due to the differing probability of a flaw being present at the filler surface. With the “strong” fillers the particle size at constant volume fraction does not alter K_{IC} .

It is interesting to note that for the dolomite composites the relationship between the yield stress and the volume fraction of filler is completely different to that for silica and alumina. As demonstrated in Fig. 1 the yield stress was constant with increasing volume fraction of dolomite whereas for alumina and silica the yield stress was considerably increased. There appears to be a correlation between the dependences of K_{IC} on volume fraction on the one hand and σ_y on volume fraction on the other, but the precise nature of this correlation is unclear at present.

References

1. C. B. BUCKNALL, *Adv. Polymer. Sci.* 27 (1978) 121.
2. L. HOLLIDAY and J. D. ROBINSON, in “Polymer Engineering Composites”, edited by M. O. W. Richardson (Applied Science, London, 1977) Ch. 6.

3. R. SCHMID and R. STIERLI, *Chimia* **19** (1965) 359.
4. L. E. NIELSEN, "Mechanical Properties of Polymers and Composites", Vol. 2 (Marcel Dekker, New York 1974) Ch. 7.
5. E. H. CHIU and J. A. MANSON, *J. Polymer Sci.* **41** (1973) 95.
6. Y. S. LIPATOV and F. G. FABULYAK, *J. Appl. Polymer Sci.* **16** (1972) 2131.
7. I. GALPERIN, *ibid.* **11** (1969) 1475.
8. H. S. KATZ and J. V. MILEWSKI, "Handbook of Fillers and Reinforcements for Plastics" (Van Nostrand Reinhold, New York, 1978).
9. K. L. TRACHTE and A. T. DIBENEDETTO, *Int. J. Polym. Mater.* **1** (1971) 75.
10. E. R. FULLER, *ATSM Spec. Tech. Publ.* **678** (1979) 3.
11. B. J. PLETKA, E. R. FULLER and B. G. LOEPKE, *ibid.* **678** (1979) 19.
12. B. STALDER and H. H. KAUSCH, *J. Mater. Sci.* **17** (1982) 2481.
13. A. G. EVANS, *ibid.* **7** (1971) 1137.
14. B. STALDER and Ph. BEGUELIN, Fifth International Conference on Deformation, Yield and Fracture of Polymers, March, 1982, Cambridge, UK (Plastics and Rubber Institution, London, 1981).
15. J. G. WILLIAMS and H. FORD, *J. Mech. Eng. Sci.* **6** (1964) 7.
16. R. W. DAVIDGE and G. TAPPIN, *J. Mater. Sci.* **3** (1968) 165.
17. C. TOURENQ and F. GRAGGER, *Naturstein Industrie* **11** (7/8) (1965) 19.
18. S. M. WIEDERHORN, *J. Amer. Ceram. Soc.* **52** (1969) 99.
19. H. G. TATTERSALL and G. TAPPIN, *J. Mater. Sci.* **1** (1966) 296.
20. R. A. GLEDHILL, A. J. KINLOCH, S. YAMINI and R. J. YOUNG, *Polymer* **19** (1978) 574.
21. A. J. KINLOCH and J. G. WILLIAMS, *J. Mater. Sci.* **15** (1980) 987.
22. Y. YAMINI and R. J. YOUNG, *ibid.* **15** (1980) 1814.
23. L. J. BROUTMAN and S. SAHU, *Mater. Eng. Sci.* **8** (1971) 98.
24. J. C. HAMMOND and D. C. QUAYLE, "Fracture energy studies of a Polyester Resin containing microspheres", 2nd International Conference on Deformation, Yield and Fracture of Polymers, March, 1973, Cambridge, UK (Plastics and Rubber Institution, London, 1973).
25. S. KUNZ-DOUGLASS, P. W. R. BEAUMONT and M. F. ASHBY, *J. Mater. Sci.* **15** (1980) 1109.
26. F. F. LANGE, *Phil. Mag.* **22/179** (1970) 983.
27. *Idem*, *J. Amer. Ceram. Soc.* **54** (1971) 614.
28. M. NARKIS, *J. Appl. Polymer Sci.* **22** (1978) 2391.
29. J. A. MANSON and L. H. SPERLING, in "Polymer Blends and Composites" (Plenum Press, New York, 1976) Ch. 12.
30. O. ISHAI and L. J. COHEN, *Int. J. Mech. Sci.* **9** (1967) 539.
31. R. J. YOUNG and P. W. R. BEAUMONT, *J. Mater. Sci.* **10** (1977) 1343.
32. *Idem*, *ibid.* **12** (1975) 684.
33. A. G. EVANS, *Phil. Mag.* **26** (1972) 1327.
34. K. C. RADFORD, *J. Mater. Sci.* **6** (1971) 1286.
35. D. J. GREEN, P. S. NICHOLSON and J. D. EMBERY, *J. Mater. Sci.* **14** (1979) 1657.
36. F. F. LANGE and K. C. RADFORD, *ibid.* **6** (1971) 1197.

*Received 15 April
and accepted 29 June 1982*